Hindawi
Advances in Civil Engineering
Volume 2022, Article ID 8780927, 11 pages
https://doi.org/10.1155/2022/8780927

Research Article

Full-Scale Laboratory Test of Cutting Large-Diameter Piles Directly by Shield Cutterhead

Yuqing Wang,[1] Xinyu Wang,[2] Yangyang Xiong,[1] Zhuangzhi Yang,[1] and Jie Zhang[1]

[1]*China Railway Tunnel Group Co Ltd., Guangzhou 511458, China*
[2]*School of Civil Engineering, Henan Polytechnic University, Jiaozuo 454000, China*

Correspondence should be addressed to Xinyu Wang; wangxinyu2010@163.com

Received 22 April 2022; Revised 18 July 2022; Accepted 29 July 2022; Published 19 August 2022

Academic Editor: Ping Xiang

Copyright © 2022 Yuqing Wang et al. This is an open access article distributed under the Creative Commons Attribution License, which permits unrestricted use, distribution, and reproduction in any medium, provided the original work is properly cited.

Based on the TBM tunnel of Red Line of Tel Aviv in Israel, this paper carried out laboratory tests of shield cutting concrete and reinforced concrete piles and investigated cutting performance of cutter, failure model of rebars, length of damaged rebars, and cutter vibration. The results indicate that under the condition of low tunneling speed and rotating speed, vibration of the cutterhead is small, and vibration of the center cutterhead is more obvious in the radial direction of the cutterhead. Cross sections of broken rebars mainly consist of shear section, tensile-shear section, tensile-compressive section, and bending section. Considering the tunnel status, it is recommended to adopt excavation speed of 3~5 mm/min, and rotating speed of 1.0~1.3 r/min. While cutting RC piles, the principle of "low excavation speed, high rotating speed, and less disturbance" is recommended. Cutting with disc cutters is efficient and the torque of which is stable but the length of the rebars got from cutting varies a lot. It is recommended that majorities of the cutters shall be disc cutters and supplemented with drag bits and tear cutters.

1. Introduction

In order to solve the problem of traffic congestion and make full use of the underground space, subway/metro tunnels have been constructed in cities worldwide. Due to the complex construction environment in cities and limitations of alignment planning of the tunnel, tunnels adjacent to the existing piles of buildings appear frequently [1–4]. In particular cases, tunnels are passing through the existing piles [5–7]. The shield tunneling method is widely used in tunnel engineering, for its advantage of safety, efficiency, high mechanization degree, and small disturbance. Compared to the methods of tunnel rerouting and pile underpinning [6, 8], cutting the piles directly using the shield cutter is more economical and efficient when shield tunnels pass through the existing reinforced concrete (RC) piles, and it has wide application prospects. During the process of shield cutting piles, parameters configuration of cutter and shield working is crucial. Therefore, it is important to execute laboratory or field tests of cutting RC piles by shield cutterhead before practical engineering application.

In recent years, most studies mainly focus on the effects of shield tunneling on existing pile foundation [1, 2, 9–14], and report related to cutting the RC piles by shield is few. Based on the construction of Suzhou metro in China, field test of shield cutting RC piles was carried out, wear and damage of the modified rippers were studied by Li et al. [7]. Wang et al. [15–17] presented a field test on shield cutting of obstacle piles, and the shield working parameters were analyzed. Based on the construction of shield cutting of bridge piles, Yuan et al. [18] studied feasibility of a new style cutter for shield cutting large-diameter RC Piles. Field test of shield cutting was presented by Chen et al. [19] to investigate variation characteristics and cutting parameters. Du et al. [20] and Xu et al. [21] executed laboratory tests of direct cutting RC piles by shield cutterhead, combination scheme of disc and tearing cutters, and reasonable cutting parameters were proposed.

Cutting the piles directly using the shield has been used in some practical engineering. However, as an emerging technology, cutting the RC piles directly by shield is not mature yet. The shield cutter which is specifically used to cut

the obstacle RC piles is still absent. Variation characteristics of cutter and cutting parameters are still in the exploratory stage and phenomena of cutter wear and cutterhead wound by rebar are widespread in practical engineering.

Based on the TBM tunnel of Red Line of Tel Aviv in Israel, laboratory tests of shield cutting concrete and reinforced concrete piles were carried out, cutting performance of cutter, failure model of rebars, length of damaged rebars, and cutter vibration were investigated through the TBM comprehensive experimental platform, thus to provide reasonable cutting parameters for cutting pile foundation in the TBM tunnel segment.

2. Project Overview

Red Line of Tel Aviv LRT project (Western Segment) is located in center of Tel Aviv in Israel. TBM tunnel (Western Segment) located between Herzl Street and Ben Gurion station is the major part of the underground works, as shown in Figure 1. It consists of twin-bore single-track tunnels with segmental lining with an inside diameter of 6.5 m having a total length of approximately 5.5 km. The shield with a diameter of 7.54 m, a maximum thrust force of 55000 kN, a nominal torque of 12000 kN·m, and a maximum rotating speed of 3.8 r/min is adopted to build the tunnel.

TBMs will be launched a Herzl shaft, then bore through Allenby station, and be lifted out at Karlibach station. The tunnels will underpass the Ayalon river and the railway tracks (Figure 2) between the Galei Gil shaft and the Arlozorov station. On both sides of the Ayalon river bed, Ayalon retaining wall structures are located. The eastern retaining wall is located about 20 m from the Galei Gil launching shaft and supports Ayalon North highway. The western retaining wall supports the railway tracks and is located about 30 m from the Galei Gil launching shaft. These retaining walls are partially supported by piles, as described in detail in the next clause. The TBM will encounter these obstacles immediately after launching. On the west bank of the river, an L-shape reinforced concrete retaining wall on pile shafts foundations was constructed, the foundation of this wall consists of two rows of piles with a diameter of 1 m and 12 m in depth. And pile foundations intruded into the tunnel are listed in Table 1.

3. Experiment Design

In order to verify the performance of shield cutter in directly cutting square and circular piles, disc cutters are installed on the cutter head and square and circular piles are symmetrically arranged in the rock disc. The pile foundation is made of C35 grade concrete, and M5 grade cement mortar is filled between the square and the circular piles.

The parameters measured in the experiment mainly include the performance of the cutter in cutting circular and square piles, the vibration characteristics of the cutters, the failure form of the steel bars, and the shield tunneling parameters. On this basis, the feasibility of cutting circular and square piles by cutter is evaluated.

3.1. Arrangement of Cutters. Fourteen 17-inch cutters with a constant cross-section are adopted in both working conditions, including six double-edge cutters (1#-6#) and eight single-edge cutters (7#-14#), as shown in Figure 3.

3.2. Arrangement of Piles in Rock Disc. In the experiment, piles are similar to Ayalon River piles that TBM#6 and TBM# 5 will be encountered. In order to simulate Ayalon piles, the circle-section pile and the square-section pile are paralleled and placed to be cast. The diameter and reinforcement of the circle-section pile and the square-section pile are approximately the same as Ayalon piles.

The diameter of the rock disc of the TBM comprehensive platform [22] is 2500 mm, the cutting diameter of the cutter is 2280 mm and the thickness of the simulated rock layer is 500 mm. The square and circular piles are arranged in parallel in the same rock disc at a ratio of 1 : 1. The circular piles form a structure with a diameter of 1200 mm and the square piles with a size of 450 mm × 400 mm. The two structures are symmetrically arranged in the disc, spaced at 280 mm. The main reinforcement bars of the circular and square piles are made of Φ25 threaded steel, and the stirrups are Φ12 plain round bars.

In order to simulate the condition, where the piles are buried deep and the built-in steel bars extend longer, the main bars and stirrups are welded and fixed during the experiment, and the top of the piles is covered with a 50 mm-thick test tunneling layer. The circular and square piles are arranged in the rock disc as shown in Figure 4.

3.3. TBM Comprehensive Experimental Platform. The TBM comprehensive experimental platform [22] of the State Key Laboratory of Shield Machine and Boring Technology is adopted in the experiment, as shown in Figure 5. The TBM comprehensive experimental platform mainly consists of a mechanical structure, hydraulic pump station, tunneling device, rotating device, spiral conveyer, and its control system. It is used either vertically or horizontally to conduct experiments on various concrete samples with its cutters made of different materials and at different cutter spacings, cutting speeds, and feed rates. Based on these statistics, the cutting efficiency and cutter service life are analyzed, thus providing cutters of appropriate material with appropriate arrangements for different projects. The experimental parameters of the TBM comprehensive experimental platform are listed in Table 2.

4. Experiment Results Analysis

4.1. Parameters of TBM Comprehensive Platform

4.1.1. Initial Value of Force on Cutter. Figure 6 shows the data of the total thrust and penetration speed of the cutters before they contact the rock disc (idle thrust). In this stage, the piles have not been cast by the cutters, and the trends of the tunneing speed can be divided into two periods: (1) From the period of 9 : 44 : 03 to 9 : 45 : 21, the maximum

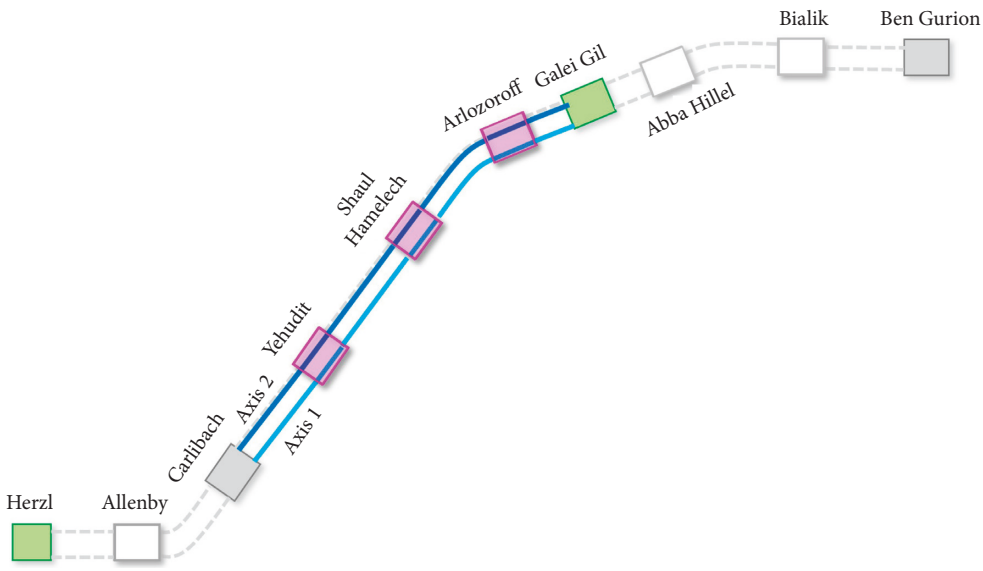

Figure 1: Red line.

Figure 2: Aylalon river.

penetration speed fed back by the cutter head is 53.7 mm/min, and the maximum thrust reaches 1778.2 kN. When the penetration speed of the cutters is controlled at 50.7–53.7 mm/min, it is generally positively correlated with the total thrust. The total thrust increases with the increase of the penetration speed control value and then remains stable at 1765.6–1778.2 kN. (2) At the period of after time 9 : 45 : 21, when the penetration speed of the cutters sharply decreases from 53.7 mm/min to zero at the time of 9 : 45 : 21, the total thrust would not decrease as rapidly. After time 9 : 45 : 21, the total thrust firstly decreases from 1778.2 kN at the time of 9 : 45 : 21 to 1465.4 kN at the time of 9 : 45 : 47. Then, it remains stable at 1595.8–1637.6 kN with increasing penetration speed of the cutters.

The cutters stop penetrating forward and are in an idling state. By controlling the rotating speed at 0.36–0.48 r/min, the torque fluctuates at 28.4–30.2 kN·m. Figure 7 shows the torque and rotating speed under idling conditions.

4.1.2. Cutting of Concrete Layer by Cutters. Set the penetration speed of the cutters. The average feedback value is 9.47 mm/min and the rotating speed is 0.61 r/min. The total thrust and torque when cutting the concrete layer are shown in Figure 8. It can be seen that the total thrust and torque of the cutters gradually increase at the constant penetration speed and rotating speed mentioned above, and the two parameters are strongly correlated.

Figure 9 shows the variation of the feedback values of cutter penetration and rotating speed when cutting the concrete layer. As can be seen from the figure, due to the step characteristics of the cutter in concrete breaking, the vibration amplitude of penetration varies greatly, ranging from 0 mm/min to 38.78 mm/min. Compared with the set value, the cutter torque varies little, ranging from 0.516 kN·m to 0.662 kN·m.

However, the cutter penetration speed and rotating speed mentioned above cannot meet the requirements for stable and efficient concrete breaking, and it is necessary to increase the rotating speed or change the penetration speed.

Increase the penetration speed, The average feedback value is 17.25 mm/min. The variation of total thrust and torque over time is shown in Figure 10. It can be found that when the penetration speed is increased, the total thrust and torque grow rapidly. The instantaneous maximum total thrust reaches 3862.5 kN, and the instantaneous maximum torque reaches 387.1 kN·m. When driving at the maximum penetration speed for a moment, the cutters get stuck and gradually stop rotating, and the torque gradually decreases to 0.

Set the penetration speed. The average feedback value is 6.47 mm/min. After the rotating speed of the cutters is increased to 1.03 r/min, the variation of the total thrust and torque over time is shown in Figure 11. As demonstrated in this figure, when the rotating speed of the cutters is increased, the total thrust and torque first increase rapidly and then decrease slowly, indicating that compared to a higher

Table 1: Pile foundations intruded into the tunnel.

Diameter (m)	Length (m)	Space (m)	Concrete grade	Length of the pile intruded into the tunnel (m)	Number of the pile intruded into the tunnel
1.2	12	2.8	B40	7.84	2
1	12	4.7	B40	7.14	1
1	13.5	1.1	B40	1.7	6

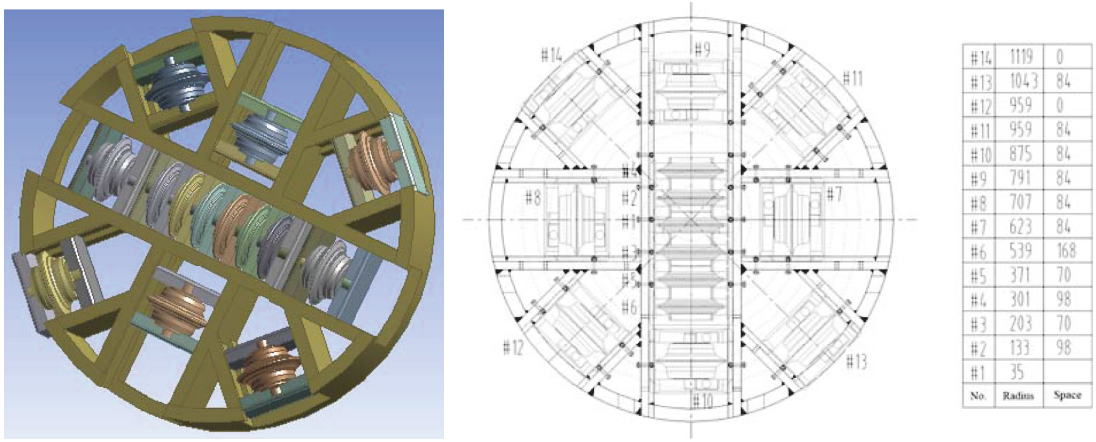

Figure 3: Arrangement of cutters.

Figure 4: Arrangement of circular and square piles in rock disc.

Figure 5: TBM comprehensive experimental platform.

rotating speed, a lower penetration speed results in lower efficiency of concrete breaking and a lower rate of energy utilization.

4.1.3. Cutting of Reinforced Concrete Layer by Cutters. When cutting the reinforced concrete layer, the average feedback value for the penetration speed of the cutters is 10.8 mm/min, and the rotating speed is 0.54 r/min. Figure 12 shows the variation of total thrust and torque over time. As can be seen from the figure, the instantaneous maximum total thrust is 4051.9 kN, and the instantaneous maximum torque is 380.72 kN·m. When the cutters work stably for a

Table 2: Main performance parameters of TBM comprehensive experimental platform.

Parameters	Value
Overall dimensions	6880 mm × 4050 mm×5176 mm
Total weight	120T
Max. Cutting diameter	2280 mm
Mould box dimensions	φ2500 mm × 1000 mm
Torque	250 kN·m
Max. Rotating speed	6rpm
Thrust force	400T
Power	250 kW
Cutter size	431.8 mm

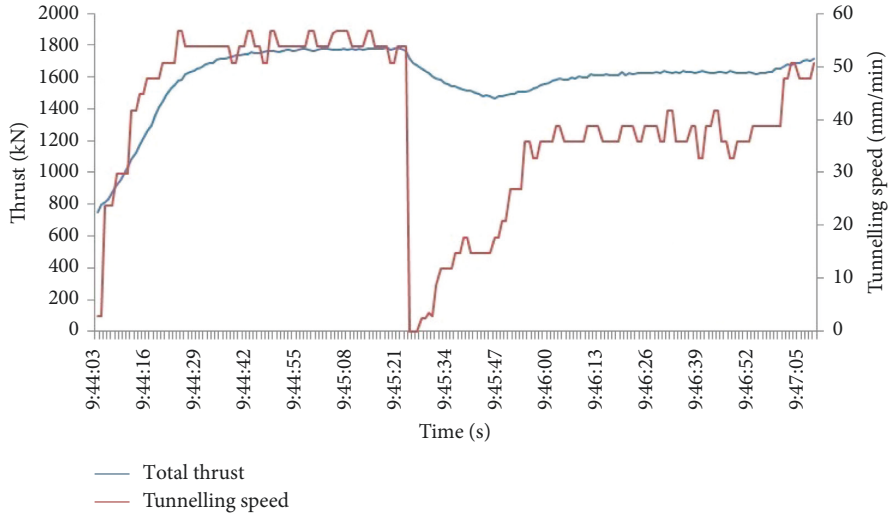

Figure 6: Variation of total thrust and penetration speed over time.

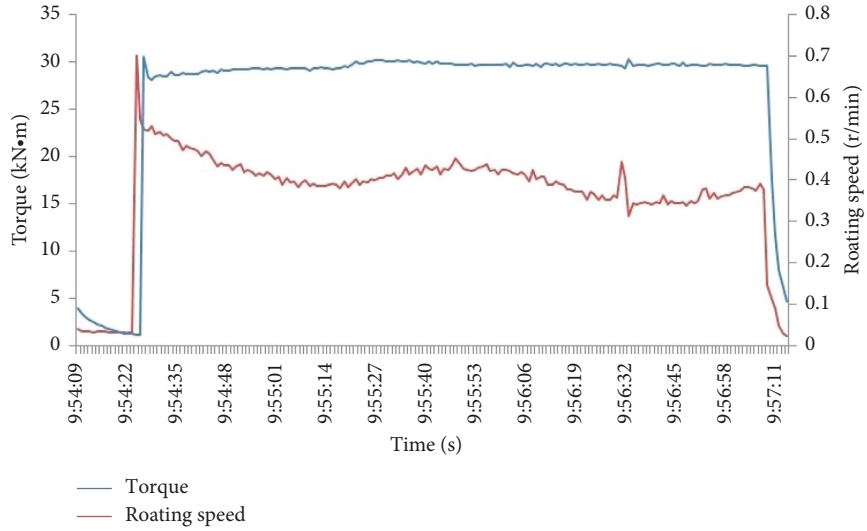

Figure 7: Variation of torque and rotating speed over time.

while, the torque reaches its maximum and the cutters get stuck, causing the torque to decrease to 0.

By comparing the thrust and torque during cutting concrete and cutting reinforced concrete (Table 3), it can be found that the thrust and torque needed for cutting concrete are apparently less than those for cutting the rebar layer. Through observation (of noise and vibration) during the test and monitoring of parameters, to ensure efficient excavation

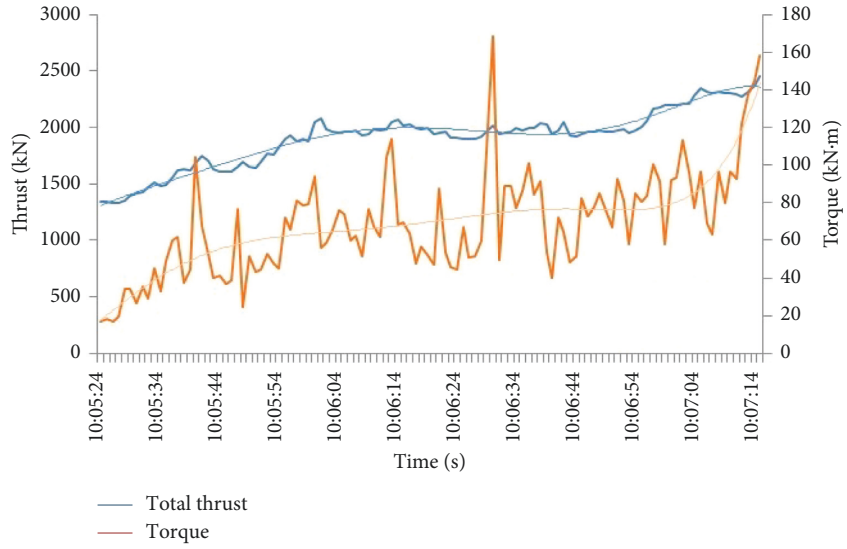

Figure 8: Variation of total thrust and torque over time.

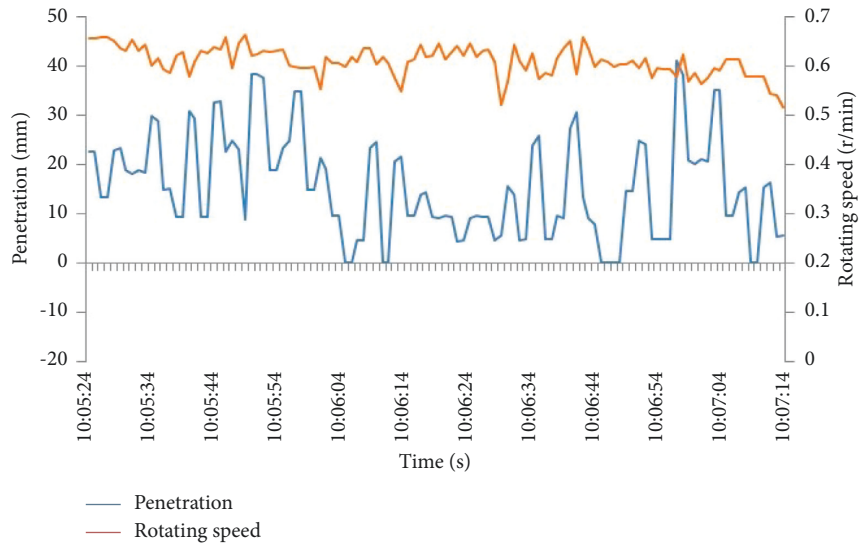

Figure 9: Variation of feedback values of penetration and rotating speed over time.

and to avoid stuck of the machine, the most appropriate parameters for cutting C35 concrete with disc cutters are 9.47 mm/min ≦ penetration speed ≦ 17.25 mm/min and rotating speed ≦0.61 r/min; for the reinforced concrete, the penetration speed shall be around 8.36 mm/min and no more than 13.30 mm/min. Certainly, increasing the rotating speed could make a higher penetration speed, so it is suggested to set the rotating speed to slightly more than 1.0 r/min.

4.2. Failure Modes of Rebars

4.2.1. Bending Forms of Rebars. Figure 13 shows some of the rebars in the reinforced concrete cut by the cutters. As can be seen from the figure, there are many long rebars in the cut ones, and some of them are severely bent. This is due to the following three reasons: (1) the rebars are not welded firmly at the ends and the welded points break apart under tensile force when cut by the cutters; (2) the concrete strength is low and is in complicated stress state, which causes the cutter force on the rebars to be transferred to the concrete, resulting in the breaking of the concrete directly under the rebars [23]. Meanwhile, the rebars deform greatly due to compression but their loss of tensile strength is small; and (3) after the ends of the rebars are broken, the rebars are continuously twisted and deformed under the rotation of the cutters.

4.2.2. Cross Section of Broken Rebars. Cross-section types of the rebars broken by the cutters mainly include shear

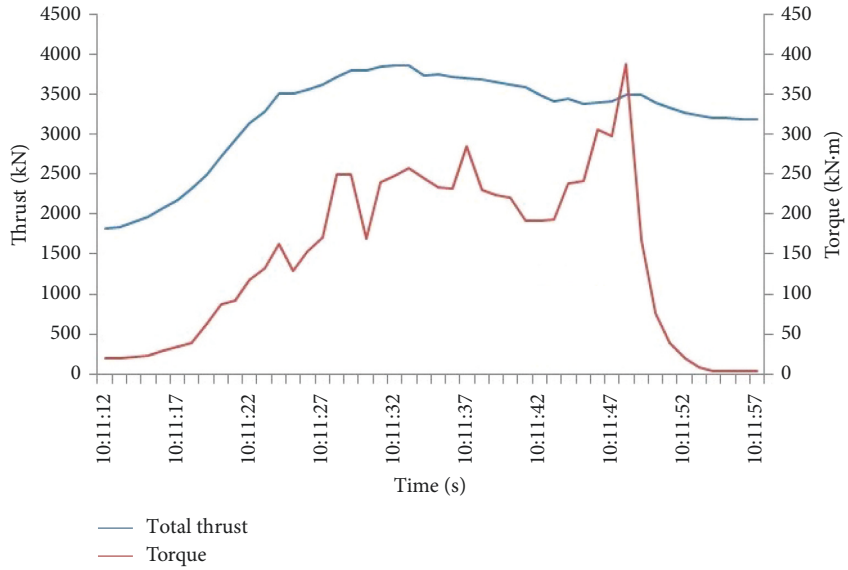

Figure 10: Variation of total thrust and torque over time.

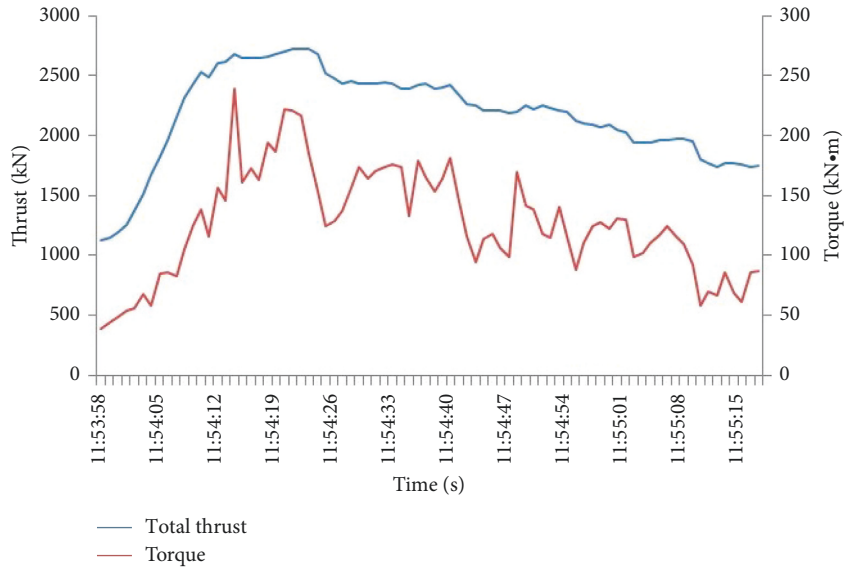

Figure 11: Variation of total thrust and torque over time.

section, tensile-shear section, tensile-compressive section, and bending section, as shown in Figure 14. Among them, the shear section is caused by the relative displacement between the rebar directly under the cutter and the one on its side under compression of the cutter. This type of cross section is smooth and reflective, with an obvious sign of one-way movement and accounting for 20% of the total countable sections. The tensile-shear section is caused by the combined action of the tensile stress of the rebar and the shear stress of the cutter. With a sign of one-way movement, it is granular and not smooth, accounting for 30% of the total countable sections. The tensile-compressive section is caused by the combined action of compression and tensile stress on the rebar. Featured by a smaller section area and a granular surface, it accounts for 10% of the total countable sections. The bending section is caused by brittle fracture of the weak surface such as cracks due to bending of the rebar under rotation of the cutter. This type accounts for 40% of the total countable sections.

4.2.3. Length of Damaged Rebars. Statistics of damaged rebars from the testing of cutting C35 reinforced concrete with disc cutters are shown in Figure 15. The damaged rebars include (1) the rebars on both sides damaged by disc cutters, and (2) the rebars damaged by disc cutters on one side and

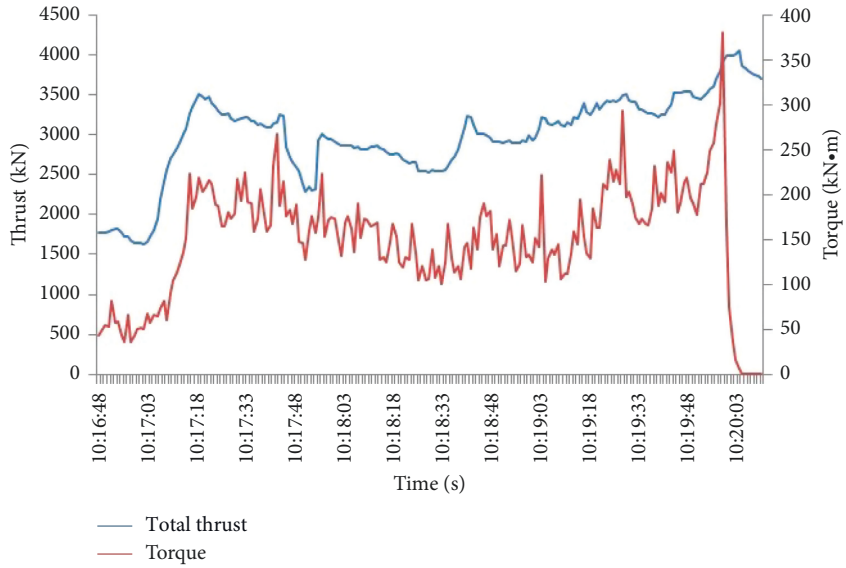

Figure 12: Variation of total thrust and torque over time.

Table 3: Test results for cutting C35 reinforced concrete layer with disc cutters.

Position of cut	Penetration speed (mm/min)	Rotating speed (r/min)	Total thrust (kN)		Torque (kN·m)		Evaluation of test results
			Ave.	Max.	Ave.	Max.	
Concrete layer	9.47	0.61	1942	—	72	—	No stuck, low efficiency
	17.25	0.61	—	3862	—	387	Stuck
Reinforced concrete layer	6.47	1.03	—	2500	—	200	No stuck, low efficiency
	8.36	0.57	2980	3512	206	275	Relatively stable
	13.30	0.51	3200	4052	200	381	Stuck

Figure 13: Rebars in the reinforced concrete cut by the cutters.

damaged between the welded points on the other side. Both sides of the rebars damaged by disc cutters shall be deemed as countable.

It could be concluded from the figure that countable rebars with a length within 0–600 mm constitute 76.92% of the total amount. Countable rebars with a length of more than 1000 mm are of 14.29% of the total amount, which could be argued that after cutting one side of the rebar, stress is released and thus disc cutters make less damage to the rebars. The rebars are not cut off but twisted, so the shrink of the cross-section is less, making it harder to cut.

4.3. Vibration of Cutters. Table 4 shows the vibration of cutters during the test. It can be seen that when cutting the concrete layer at low excavation speed and low rotating

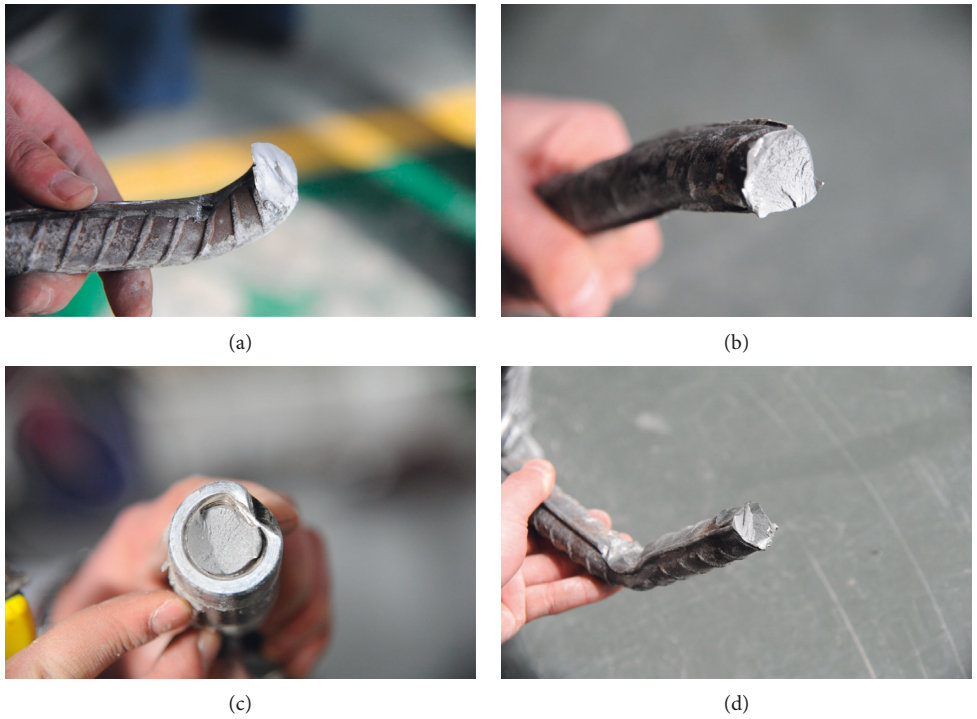

Figure 14: Cross section of broken reinforcement. (a) Shear section; (b) Tensile-shear section; (c) Tensile-compressive section; and (d) Bending section.

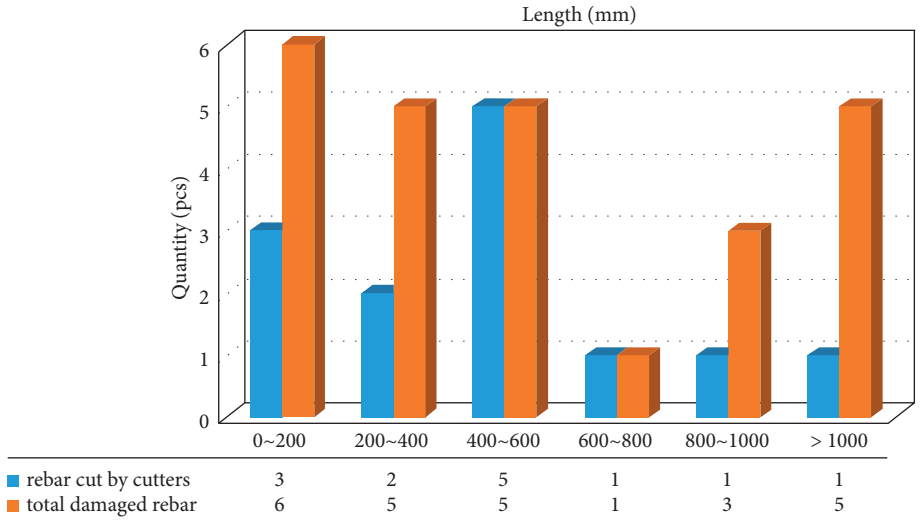

Figure 15: Length of damaged rebars.

Table 4: Vibration of the cutters.

Position of cut	Center cutter holder		9# cutter holder
	Axial vibration acceleration of cutter (g)	Radial vibration acceleration of cutter (g)	Circumferential vibration acceleration of cutter (g)
Concrete layer	−0.563–0.495	−0.929–1.077	—
Reinforced concrete layer	−0.952–1.272	−3.714–3.084	−2.188–1.556

Figure 16: Cutters after test.

speed, the vibration acceleration of the center cutter holder is -0.929~1.077 g in the radial direction of the cutter and -0.563~0.495 g in the axial direction of the cutter.

When cutting the reinforced concrete layer, the center cutter holder vibrates violently with an acceleration of -3.714~3.084 g in the radial direction of the cutter, and an acceleration of -0.95 g~1.272 g in the axial direction of the cutter. The vibration acceleration of the 9# cutter holder is -2.188~1.556 g in the circumferential direction of the cutter. Based on the analysis abovementioned, it can be concluded that for the structural design of the TBM comprehensive platform, when cutting the reinforced concrete layer, the vibration of the center cutters is strongest and then weakens as it goes outward.

4.4. Wear of Cutters. As the C35 reinforced concrete layer cut by the cutters is only 500 mm thick, the wear of the cutters cannot be measured. The cutters used in the test are brand new 27-inch cutters provided by China Railway Engineering Equipment Group Co., Ltd. Figure 16 shows the cutters after cutting the C35 reinforced concrete layer.

5. Conclusions

Based on the TBM tunnel of Red Line of Tel Aviv in Israel, laboratory tests of shield cutting concrete and reinforced concrete piles were carried out, cutting performance of cutter, failure model of rebars, length of damaged rebars, and cutter vibration were investigated through the TBM comprehensive experimental platform. Based on the results, the following conclusions could be summarized.

(1) Under the condition of low tunneling speed and rotating speed, vibration of the cutterhead is small, and vibration of the center cutterhead is more obvious in the radial direction of the cutterhead.

(2) Long rebars exist in the cut rebars, and some of them are severely bent. Cross sections of broken rebars mainly consist of shear section, tensile-shear section, tensile-compressive section, and bending section.

(3) Considering the tunnel status, it is recommended to adopt an excavation speed of 3~5 mm/min, rotating speed of 1.0~1.3 r/min. While cutting RC piles, the principle of "low excavation speed, high rotating speed, less disturbance" is recommended to increase the capability of cutting rebars.

(4) Cutting with disc cutters is efficient and torque of which is stable but the length of the rebars got from cutting varies a lot. It is recommended that majorities of the cutters shall be disc cutters and supplemented with drag bits and tear cutters.

Data Availability

All data generated or analyzed during this study are included in this published article.

Conflicts of Interest

The authors declare that they have no conflicts of interest or personal relationships that could have appeared to influence the work reported in this paper.

Acknowledgments

This work was supported by Key Program of Technology and Innovation of China Railway Tunnel Group (2016–18).

References

[1] C. Liu, Z. X. Zhang, and R. A. Regueiro, "Pile and pile group response to tunnelling using a large diameter slurry shield – case study in Shanghai," *Computers and Geotechnics*, vol. 59, pp. 21–43, 2014.

[2] C. Li, Z. L. Zhong, G. N. He, and X. R. Liu, "Response of the ground and adjacent end-bearing piles due to side-by-side twin tunnelling in compound rock strata," *Tunnelling and Underground Space Technology*, vol. 89, pp. 91–108, 2019.

[3] Y. J. Jeon, S. C. Jeon, S. J. Jeon, and C. J. Lee, "Study on the behaviour of pre-existing single piles to adjacent shield tunnelling by considering the changes in the tunnel face pressures and the locations of the pile tips," *Geomechanics and Engineering*, vol. 21, pp. 187–200, 2020.

[4] K. Huang, Y. W. Sun, D. Q. Zhou, Y. J. Li, M. Jiang, and X. Q. Huang, "Influence of water-rich tunnel by shield tunneling on existing bridge pile foundation in layered soils," *Journal of Central South University*, vol. 28, no. 8, pp. 2574–2588, 2021.

[5] T. Ishimura, M. Metoki, and M. Shimizu, "Development of removed pile method with cutting," *Tunnelling and Underground Space Technology*, vol. 21, no. 3-4, pp. 411-412, 2006.

[6] C. R. Zhang, Y. J. Zhao, Z. Zhang, and B. Zhu, "Case study of underground shield tunnels in interchange piles foundation underpinning construction," *Applied Sciences*, vol. 11, no. 4, p. 1611, 2021.

[7] X. G. Li, D. J. Yuan, X. Q. Jiang, and F. Wang, "Damages and wear of tungsten carbide-tipped rippers of tunneling machines used to cutting large diameter reinforced concrete piles," *Engineering Failure Analysis*, vol. 127, Article ID 105533, 2021.

[8] Q. W. Xu, H. H. Zhu, X. F. Ma et al., "A case history of shield tunnel crossing through group pile foundation of a road

bridge with pile underpinning technologies in Shanghai," *Tunnelling and Underground Space Technology*, vol. 45, pp. 20–33, 2015.

[9] F. Chen, C. He, X. Li, and B. Wang, "Construction schemes for shallow and asymmetrically loaded tunnels crossing below a bridge," *International Journal of Geomechanics*, vol. 20, no. 7, Article ID 04020098, 2020.

[10] Y. Q. Li and W. G. Zhang, "Investigation on passive pile responses subject to adjacent tunnelling in anisotropic clay," *Computers and Geotechnics*, vol. 127, Article ID 103782, 2020.

[11] P. L. Li, Y. Q. Lu, J. X. Lai, H. Q. Liu, and K. Wang, "A comparative study of protective schemes for shield tunneling adjacent to pile groups," *Advances in Civil Engineering*, vol. 2020, pp. 1–16, 2020.

[12] Z. Li, Z. Q. Chen, L. Wang, Z. K. Zeng, and D. G. Gu, "Numerical simulation and analysis of the pile underpinning technology used in shield tunnel crossings on bridge pile foundations," *Underground Space*, vol. 6, no. 4, pp. 396–408, 2021.

[13] Y. X. Zheng, Z. P. Hu, X. Ren, R. Wang, and E. X. Zhang, "The influence of partial pile cutting on the pile-anchor supporting system of deep foundation pit in loess area," *Arabian Journal of Geosciences*, vol. 14, no. 13, p. 1229, 2021.

[14] K. Huang, Y. W. Sun, J. He, X. Q. Huang, M. Jiang, and Y. J. Li, "Comparative study on grouting protection schemes for shield tunneling to adjacent viaduct piles," *Advances in Materials Science and Engineering*, vol. 202119 pages, Article ID 5546970, 2021.

[15] F. Wang, D. J. Yuan, C. W. Dong, B. Han, H. R. Nan, and M. S. Wang, "Study on cutter configuration for directly shield cutting of large-diameter piles," *China Civil Engineering Journal*, vol. 46, no. 12, pp. 127–135, 2013.

[16] F. Wang, D. J. Yuan, C. W. Dong, B. Han, H. R. Nan, and M. S. Wang, "Test study of shield cutting large-diameter reinforced concrete piles directly," *Chinese Journal of Rock Mechanics and Engineering*, vol. 32, no. 12, pp. 2566–2574, 2013.

[17] Y. L. Wang, J. C. Li, and S. M. Liao, "Numerical simulation and measured data analysis of pile group cutting by shield: a case study of running tunnel on line No. 9 of Shenzhen metro," *Tunnel Constrction*, vol. 37, no. 2, pp. 192–199, 2017.

[18] D. J. Yuan, F. Wang, C. W. Dong, B. Han, and M. S. Wang, "Study on new-style cutter for shield cutting large-diameter reinforced concrete pile," *China Journal of Highway and Transport*, vol. 29, no. 3, pp. 89–97, 2016.

[19] H. F. Chen, D. J. Yuan, F. Wang, and M. S. Wang, "Study on shield cutting parameters when cutting big diameter piles," *China Civil Engineering Journal*, vol. 49, no. 10, pp. 103–110, 2016.

[20] C. D. Du, J. Zhang, and Z. X. Tang, "Key technologies of shield direct cutting pile foundation," *Tunnel Constrction*, vol. 39, no. 10, pp. 1–12, 2019.

[21] H. G. Xu, K. Chen, and Z. C. Sun, "Laboratory test of reinforced concrete pile foundation cutting by shield cutterhead," *Tunnel Constrction*, vol. 40, no. 1, pp. 35–42, 2020.

[22] Y. D. Yang, Z. C. Sun, F. Y. Li, B. Zhang, and H. G. Xu, "Research on upgrading of TBM boring modal experiment platform," *Tunnel Constrction*, vol. 40, no. 11, pp. 1570–1577, 2020.

[23] F. Ding, X. Wu, P. Xiang, and Z. Yu, "New damage ratio strength criterion for concrete and lightweight aggregate concrete," *ACI Structural Journal*, vol. 118, no. 6, pp. 165–178, 2021.